optica

Extreme-depth-of-focus imaging with a flat lens

Sourangsu Banerji,[1,†] Monjurul Meem,[1,†] Apratim Majumder,[1] Berardi Sensale-Rodriguez,[1] and Rajesh Menon[1,2,*]

[1]Department of Electrical and Computer Engineering, University of Utah, Salt Lake City, Utah 84102, USA
[2]Oblate Optics, Inc., San Diego, California 92130, USA
*Corresponding author: rmenon@eng.utah.edu

Received 25 November 2019; revised 3 February 2020; accepted 11 February 2020 (Doc. ID 384164); published 12 March 2020

A lens performs an approximately one-to-one mapping from the object to the image plane. This mapping in the image plane is maintained within a depth of field (or referred to as depth of focus, if the object is at infinity). This necessitates refocusing of the lens when the images are separated by distances larger than the depth of field. Such refocusing mechanisms can increase the cost, complexity, and weight of imaging systems. Here we show that by judicious design of a multi-level diffractive lens (MDL) it is possible to drastically enhance the depth of focus by over 4 orders of magnitude. Using such a lens, we are able to maintain focus for objects that are separated by as large a distance as ∼6 m in our experiments. Specifically, when illuminated by collimated light at λ = 0.85 μm, the MDL produced a beam, which remained in focus from 5 to 1200 mm. The measured full width at half-maximum of the focused beam varied from 6.6 μm (5 mm away from the MDL) to 524 μm (1200 mm away from the MDL). Since the side lobes were well suppressed and the main lobe was close to the diffraction limit, imaging with a horizontal × vertical field of view of 40° × 30° over the entire focal range was possible. This demonstration opens up a new direction for lens design, where by treating the phase in the focal plane as a free parameter, extreme-depth-of-focus imaging becomes possible.

https://doi.org/10.1364/OPTICA.384164

1. INTRODUCTION

A lens is an optical element that focuses incident collimated light into a focal spot. The distance range measured normal to the lens over which the spot remains tightly focused is generally referred to as the depth of focus (DOF). There is a direct relationship between the DOF and the focal spot size W, [1] given by

$$\mathrm{DOF} \sim \frac{4W^2}{\lambda} = \frac{\lambda}{\mathrm{NA}^2}, \tag{1}$$

where λ is the illumination wavelength and NA is the numerical aperture of the lens. When used for imaging, the images of objects outside the equivalent range in the object side will be blurry. There are obviously many reasons to extend this range for enhanced DOF imaging. This may be achieved via wavefront coding or computationally or via some combination of these [2]. Wavefront coding [3,4] and related approaches such as with a logarithmic asphere [5] generally leads to a trade-off between resolution and DOF, sometimes at the expense of image quality, primarily due to the increased side lobes. The axicon can be used to enhance DOF, but the image resolution and field of view are heavily curtailed [6,7]. Lenses with multiple discrete foci have also been demonstrated [8,9]. Optimized apodizers in the pupil plane [10] as well as binary phase optimized phase masks, by themselves [11–13] and combined with refractive lenses [14], have been used to enhance DOF. In all cases, the enhancement of DOF is relatively small, less than 1 order of magnitude. Many of these prior examples require extensive post-processing; their field of view (FOV) is heavily curtailed or requires multiple elements and tends to be quite thick. Computational enhancement of DOF also suffers from noise amplification and high sensitivity to the signal-to-noise ratio of the collected signals. Table S1 (see Supplement 1) summarizes relevant prior work in this field, from which we can conclude that the best enhancement of DOF over the diffraction limit is ∼ 600 [15], which was achieved with a fractal zone plate combined with a conventional focusing lens. In this paper, we show that with appropriate design of a flat multilevel diffractive lens (MDL), it is possible to increase the DOF to over 10^4 times than that of a diffraction-limited case as described below. The MDL is designed to focus at the diffraction limit over the entire range of $z = f_{\min}$ to $z = f_{\max}$, where z is the distance measured from the MDL [see Fig. 1(a)], and $f_{\min}$ and $f_{\max}$ are the minimum and maximum focal lengths, respectively. The NA [16] is defined as

$$\mathrm{NA} = \sin\left(\tan^{-1}\left(\frac{R}{z}\right)\right), \tag{2}$$

where $z \in (f_{\min}, f_{\max})$ and R is the radius of the MDL. In other words, the NA varies with z as expected from the diffraction limit. The largest NA of our MDL occurs at $z = f_{\min} = 5$ mm and is 0.18. The range $f_{\min} - f_{\max} = 1.2\ \mathrm{m} \sim \lambda \times 10^6$ is the new DOF, and the maximum DOF enhancement over the diffraction-limited case for this NA is $((10^6 \times \lambda)/(\lambda/\mathrm{NA}^2)) > 3 \times 10^4$, which is orders of magnitude larger than anything demonstrated before. With such a large DOF, it is possible to remove focusing mechanisms from cameras, thereby reducing cost, weight, and associated complexity.

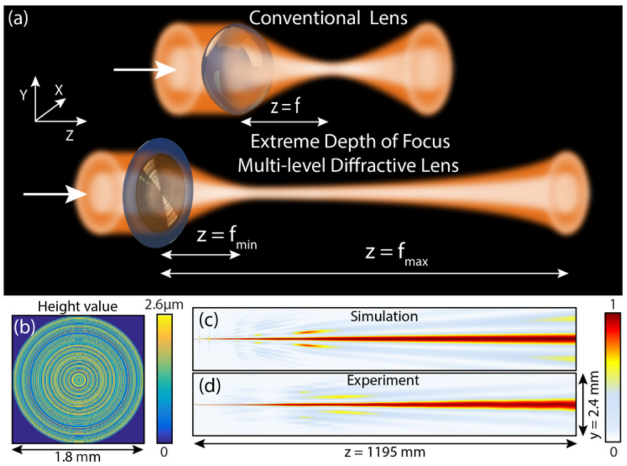

Fig. 1. (a) Schematic of a multi-level diffractive lens (MDL) that exhibits extreme-depth-of-focus (ExDOF) imaging. (b) Geometry of the MDL with focal range = 5 to 1200 mm, aperture = 1.8 mm. The (c) simulated and (d) measured intensity distributions in the $y - z$ plane for the MDL with focal lengths = 5 to 1200 mm. The operating wavelength is 850 nm.

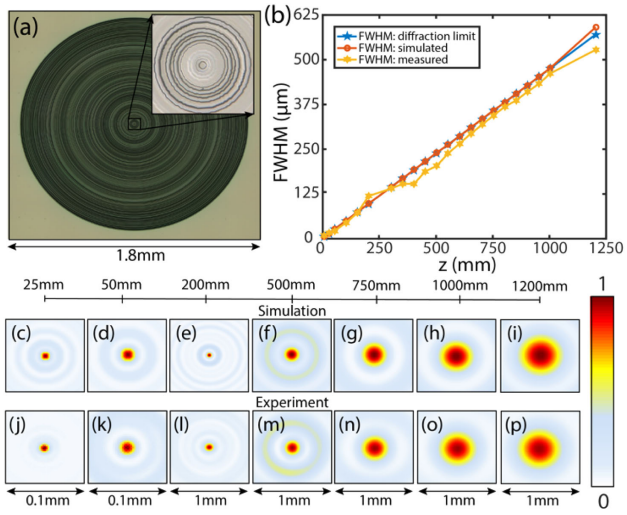

Fig. 2. (a) Optical micrograph of the fabricated MDL, with the inset showing a magnified view of the center of the lens. (b) Measured, simulated, and diffraction-limited full-width at half-maximum (FWHM) as a function of z. (c–i) Simulated and (j–p) measured point-spread functions (light intensity distributions in the $x - y$ planes) as a function of z, the distance from the MDL.

2. DESIGN

Our design methodology is inspired from our recent demonstration that for intensity imaging, phase in the focal plane could be treated as a free parameter [17]. In principle, this would enable infinite solutions to the ideal lens problem, and one can choose the desired solution based upon other requirements such as achromaticity [17,18] or enhanced DOF (in this paper). By only constraining the intensity to be focused in a large focal range and allowing the phase within this focal range to vary, we can solve a nonlinear inverse problem via optimization [17,19–25]. We choose to omit an in-depth discussion of the design methodology to keep the message of the paper simple enough to highlight the true significance of this work. Nevertheless, to summarize, we maximize the focusing efficiency of the MDL by selecting the distribution of heights of its constituent rings [see Fig. 1(b)]. In the case of our extreme-depth-of-focus (ExDOF) MDL, the focusing efficiency was defined as the ratio of power inside a spot of diameter = 3 × FWHM to the incident power, computed for each focal plane within the desired focal range. The focal range is defined as the range of distances measured from the MDL over which the light is desired to be focused [$f_{\max} - f_{\min}$ in Fig. 1(a)].

The selection of ring heights was based upon a gradient-descent-directed binary search technique [17,22,23]. The optimization routine was coupled with a conventional Fresnel–Kirchhoff diffraction integral to model the beam propagation starting from the lens plane up to the observation plane along the entire z range. A unit amplitude uniform illumination was assumed to impinge on the MDL. The MDL is polarization insensitive, and we note that all experiments here were performed with unpolarized light. We designed, fabricated, and characterized an ExDOF MDL for $\lambda = 0.85$ μm with the following parameters: $f_{\min} = 5$ mm, $f_{\max} = 1200$ mm, and aperture = 1.8 mm. The design was constrained to a ring width of 3 μm, and at most 100 height levels with a maximum height of 2.6 μm. Note that the f# (NA) varies due to the extended focus between 2.78 (0.18) and 555.56 (0.0009). The diffraction-limited DOF given by $\lambda/\max(\mathrm{NA})^2$ is 26 μm for this specific design. Therefore, the enhancement in DOF over the diffraction limit is given by

$$e_{\mathrm{DOF}} = \frac{f_{\max} - f_{\min}}{\frac{\lambda}{\max(\mathrm{NA})^2}}, \tag{3}$$

which is 3.8×10^4. This enhancement is several orders of magnitude larger than anything that has been demonstrated before, and post-processing of the images is not required. We emphasize here that we are ensuring that a single flat MDL is able to span such a large range of NAs, which, in other words, leads to an ExDOF in imaging. The diffraction limit dictates that focal spots that are farther away from the MDL will be larger.

3. RESULTS AND DISCUSSION

The light intensity distribution in the $x - z$ plane [see Fig. 1(a) for coordinate definition] was simulated and plotted for the MDL in Fig. 1(c). From the simulation, it is clear that the main lobe of the focus is maintained over the desired focal range. The FWHM of the MDL was observed to be close to the diffraction limit across the focal range. For instance, the FWHM was 524 μm at a distance of 1200 mm. The corresponding measurements are shown in Fig. 1(d). In all cases, the side lobes are also fairly well suppressed within the desired focal range, which is unlike what one would expect from a Bessel beam, for instance. This is extremely important for imaging. The material dispersion of a positive-tone photoresist, S1813 (Microchem), was assumed in the design as well as in the simulation [16]. The device was then fabricated using grayscale lithography as has been reported previously (Fig. S3 of Supplement 1) [16,18–21]. Note that due to our fabrication constraint, we were limited to a maximum ring height of 2.6 μm. An optical micrograph of the fabricated MDL is shown in Fig. 2(a).

The MDL was illuminated by a collimated beam from a supercontinuum source (NKT Photonics, SuperK EXB6) equipped with a tunable filter (NKT Photonics, SuperK SELECT) that was tuned to 850 nm with a bandwidth of 15 nm. The point-spread

function (PSF or the light intensity distribution in the $x-y$ plane) was recorded directly on a monochrome CMOS image sensor (DMM 27UP031-ML, The Imaging Source). The image sensor was placed on a stage and the PSFs were captured at different distances from the MDL (see Supplement 1 for details). After that, these images were concatenated to create the $x-z$ slice that is shown in Fig. 1(d). From these distributions, we experimentally confirmed that the incident light remains focused within the desired focal range, i.e., 5–1200 mm. We further note that the experiments agree with the simulations. The FWHM was extracted from both the simulated and measured PSFs. It is then plotted as a function of z in Fig. 2(b). The diffraction-limited FWHM is also plotted for comparison. We note the excellent agreement between all three plots. We summarize the simulated [Figs. 2(c)–2(i)] and measured [Figs. 2(j)–2(p)] PSFs for z (the distance between the MDL and the image sensor) = 25, 50, 200, 500, 750, 1000, and 1200 mm, respectively. The recorded PSFs for some of the other z values are also shown in Fig. S1 (see Supplement 1) [16]. There is good agreement between the experiments and simulations, although we believe some of the discrepancies can be attributed to expected fabrication errors (see Supplement 1). In any case, it is clear that the MDL focuses incident light close to the diffraction limit over its designed focal range. We also computed the focusing efficiency and the modulation transfer function as a function of z from the measured PSFs and summarized the data in Figs. S2 and S7, respectively (see Supplement 1).

For a conventional lens with fixed focal length (f), the object distance (u) and image distance (v) are related by the formula $1/u + 1/v = 1/f$.

If either of u or v changes, then the other has to be adjusted to capture a focused image. For example, if the object moves closer to the lens (decreasing u), then the sensor must move away from the lens (increasing v). Since the focal length of our ExDOF lens is not a fixed value, we can image objects at different distance (changing u) without necessarily moving the sensor (fixed v). The same is true for imaging the same object (fixed u) at different image distance (changing v). To illustrate this concept, we used the MDL to capture test images using the same CMOS image sensor as before. In each case, the exposure time was adjusted to ensure that the frames were not saturated. In addition, a dark frame was recorded and subtracted from the images. In all experiments, we recorded images of the Air Force resolution target under two different scenarios. First, we kept the distance between the MDL and the image sensor (v) fixed and varied the distance between the MDL and the object (u) as illustrated in Fig. 3(a). The idea was to demonstrate a camera that does not need to be refocused as u changes. The recorded images for the MDL are shown in Fig. 3(b). The values of u are noted in parentheses in each image. The experiment was repeated for three different values of v as indicated. We note that the MDL was able to form focused images for u from 50 to 1000 mm without any change in v, i.e., without having to refocus. From the recorded images, we can compute the magnification of the camera and plot it as function of u and v for the MDL in Fig. 3(c). We note that the MDL allows one to change the magnification without any change in the image distance (v). The magnification is an inverse function of u as expected from basic geometrical optics. A standard blind deconvolution was applied to improve the quality of the raw images (see Supplement 1).

In the next set of experiments, we kept u fixed and varied v, while recording the images as illustrated in Fig. 4(a). These

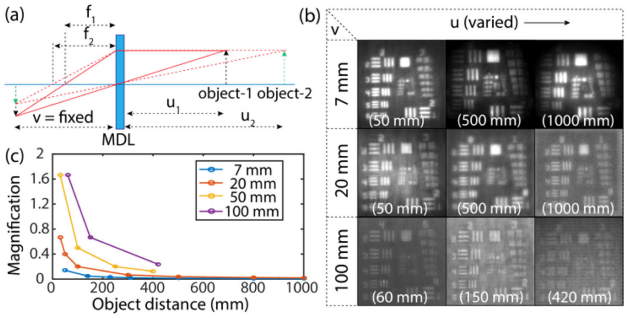

Fig. 3. Imaging different object distances without refocusing. (a) Focused images of objects at different distances u from the MDL are formed at the same image distance v. (b) Images of the Air Force resolution chart for fixed v and varying u. The value of v is fixed for each row, and the value of u is noted in parentheses in each image. (c) Magnification as a function of u for various values of v extracted from the recorded images. Imaging at different image distances without refocusing.

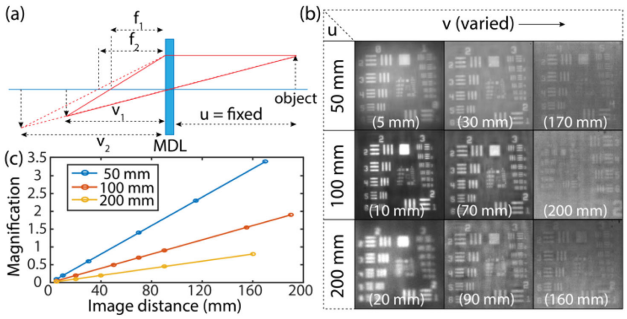

Fig. 4. (a) Focused images of objects at fixed distance u are formed at a large range of image distances v. (b) Images of the Air Force resolution chart for fixed u and varying v. The value of u is fixed for each row, and the value of v is noted in parentheses in each image. (c) Magnification as a function of v for various values of u extracted from the recorded images.

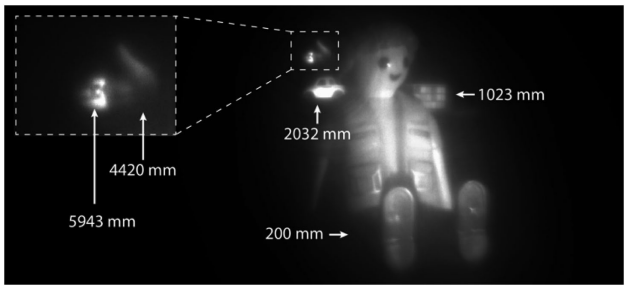

Fig. 5. Imaging a scene with large depth of field. Objects with distances from 200 mm to ~6 m are in focus. The distance of each object from the MDL (u) is noted in the figure. Video recordings of similar scenes are included as Visualization 1 and Visualization 2. A visible image of this scene is also included in Fig. S5, Supplement 1.

experiments indicate that the image of an object will remain in focus even when the image distance v is changed by a large distance. The recorded images are summarized in Fig. 4(b). We note that the MDL is able to form focused images for v from 5 to 170 mm without any change in u. The corresponding magnification was extracted and plotted as a function of v for different values of u in Fig. 4(c). Magnification is a linear function of v as expected

from basic geometrical optics. For comparison, we also repeated the same experiments in Figs. 3 and 4 with two different Fresnel lenses with focal lengths of 100 mm and 602.5 mm, respectively, and diameter = 1.8 mm (same as the MDL). The details of the experiments are given in Supplement 1 (Section 11). Not surprisingly, the conventional Fresnel lenses cannot obtain such large DOF as the MDL. For completeness, we also compared the MDL focusing performance to that of an aperture of the same diameter as the MDL (see Fig. S19). Expectedly, the aperture has no focusing power.

Finally, in order to demonstrate the imaging potential of our MDL, we imaged a scene containing objects spanning a large DOF from 200 to 5943 mm (see Fig. 5). A conventional lens will not be able to keep all the objects in focus over such a large DOF. However, the MDL is able to take a single image where all the objects are in focus (see Section 5 of Supplement 1 for details). Images of this scene were also taken with a conventional lens emphasizing its reduced DOF (Fig. S12 of Supplement 1).

4. CONCLUSIONS

The DOF is a fundamental property of a lens. By recognizing that the lens is primarily used for intensity imaging, we can treat the phase in the image (or focal) plane as a free parameter. Thereby, we can generate a phase-only pupil function that when imprinted on a beam results in a focus that can remain close to diffraction limited over a distance that is orders of magnitude larger than that of the conventional lens. We demonstrate, with an example of a pupil function modelled as a multi-level diffractive lens, a beam focused from 5 to 1200 mm. Furthermore, we also imaged scenes with objects spread as far apart as almost 6 m, where all such objects were in focus. By following this design philosophy, we believe that entirely new types of planar optics with large bandwidths, large DOF, and so on will be attainable. Finally, we also emphasize that the parameters of our optical system do not satisfy the Fraunhofer (far-field) approximation, which requires $(D^2/(f_{max} \times \lambda)) \ll 1$, where D denotes the aperture diameter of the MDL. In our MDL, this is equal to 3.17, and therefore our system lies in the Fresnel diffraction regime.

Funding. National Science Foundation (ECCS 1828480, ECCS 1936729); Office of Naval Research (N66001-10-1-4065).

Acknowledgment. We thank Brian Baker, Steve Pritchett, and Christian Bach for fabrication advice, and Tom Tiwald (Woollam) for measuring dispersion of materials. The support and resources with the computing facilities from the Center for High Performance Computing at the University of Utah and Amazon Web Services Award 051241749381 are gratefully acknowledged.

Disclosures. R. M.: Oblate Optics, Inc. (I, P, R).

See Supplement 1 for supporting content.

[†]These authors contributed equally to this work.

REFERENCES

1. M. Born and E. Wolf, *Principle of Optics*, 7th ed. (Cambridge University, 1999).
2. Z. Zalevsky, SPIE Rev. **1**, 018001 (2010).
3. E. R. Dowski and W. T. Cathey, Appl. Opt. **34**, 1859 (1995).
4. W. T. Cathey and E. R. Dowski, Appl. Opt. **41**, 6080 (2002).
5. W. Chi and N. George, Opt. Lett. **26**, 875 (2001).
6. J. M. Mcleod, J. Opt. Soc. Am. **50**, 166 (1960).
7. J. W. Y. Lit and R. Tremblay, J. Opt. Soc. Am. **63**, 445 (1973).
8. R. Hans, "Multiple focal length lens," US patent 3,004,470 (17 October 1961).
9. J. Sochacki, Appl. Opt. **23**, 4444 (1984).
10. J. Ojeda-Castañeda, E. Tepichin, and A. Diaz, Appl. Opt. **28**, 2666 (1989).
11. H. Wang, L. Shi, B. Lukyanchuk, C. Sheppard, and C. T. Chong, Nat. Photonics **2**, 501 (2008).
12. A. Kolodziejczyk, S. Bara, Z. Jaroszwicz, and M. Zypek, J. Mod. Opt. **37**, 1283 (1990).
13. Z. Liu, A. Flores, M. R. Wang, and J. J. Yang, Proc. SPIE **5783**, 841 (2005).
14. A. Flores, M. R. Wang, and J. J. Yang, Appl. Opt. **43**, 5618 (2004).
15. Q. Q. Zhang, J. G. Wang, M. W. Wang, J. Bu, S. W. Zhu, R. Wang, B. Z. Gao, and X. C. Yuan, J. Opt. **13**, 055301 (2011).
16. S. Banerji, M. Meem, A. Majumder, F. Vasquez-Guevara, B. Sensale-Rodriguez, and R. Menon, Opt. Lett. **44**, 5450 (2019).
17. S. Banerji, M. Meem, A. Majumder, B. Sensale-Rodriguez, and R. Menon, "Imaging over an unlimited bandwidth with a single diffractive surface," arXiv: 1907.06251 [physics.optics] (2019).
18. S. Banerji, M. Meem, A. Majumder, F. G. Vasquez, B. Sensale-Rodriguez, and R. Menon, Optica **6**, 805 (2019).
19. P. Wang, N. Mohammad, and R. Menon, Sci. Rep. **6**, 21545 (2016).
20. N. Mohammad, M. Meem, B. Shen, P. Wang, and R. Menon, Sci. Rep. **8**, 2799 (2018).
21. M. Meem, A. Majumder, and R. Menon, Opt. Express **26**, 26866 (2018).
22. M. Meem, S. Banerji, A. Majumder, F. G. Vasquez, B. Sensale-Rodriguez, and R. Menon, Proc. Nat. Acad. Sci. **116**, 21375 (2019).
23. S. Banerji and B. Sensale-Rodriguez, Sci. Rep. **9**, 5801 (2019).
24. S. Banerji and B. Sensale-Rodriguez, Proc. SPIE **10982**, 109822X (2019).
25. S. Banerji, M. Meem, A. Majumder, C. Dvonch, B. Sensale-Rodriguez, and R. Menon, OSA Continuum **2**, 2968 (2019).